



Event-shape and multiplicity dependence of freeze-out radii in pp collisions at root s=7 TeV

Alice Collaboration

Published in:
Journal of High Energy Physics

DOI:
[10.1007/JHEP09\(2019\)108](https://doi.org/10.1007/JHEP09(2019)108)

Publication date:
2019

Document version
Publisher's PDF, also known as Version of record

Citation for published version (APA):
Alice Collaboration (2019). Event-shape and multiplicity dependence of freeze-out radii in pp collisions at root s=7 TeV. *Journal of High Energy Physics*, 2019(9), [108]. [https://doi.org/10.1007/JHEP09\(2019\)108](https://doi.org/10.1007/JHEP09(2019)108)

Event-shape and multiplicity dependence of freeze-out radii in pp collisions at $\sqrt{s} = 7$ TeV



ALICE

The ALICE collaboration

E-mail: ALICE-publications@cern.ch

ABSTRACT: Two-particle correlations in high-energy collision experiments enable the extraction of particle source radii by using the Bose-Einstein enhancement of pion production at low relative momentum $q \propto 1/R$. It was previously observed that in pp collisions at $\sqrt{s} = 7$ TeV the average pair transverse momentum k_T range of such analyses is limited due to large background correlations which were attributed to mini-jet phenomena. To investigate this further, an event-shape dependent analysis of Bose-Einstein correlations for pion pairs is performed in this work. By categorizing the events by their transverse sphericity S_T into spherical ($S_T > 0.7$) and jet-like ($S_T < 0.3$) events a method was developed that allows for the determination of source radii for much larger values of k_T for the first time. Spherical events demonstrate little or no background correlations while jet-like events are dominated by them. This observation agrees with the hypothesis of a mini-jet origin of the non-femtoscopic background correlations and gives new insight into the physics interpretation of the k_T dependence of the radii. The emission source size in spherical events shows a substantially diminished k_T dependence, while jet-like events show indications of a negative trend with respect to k_T in the highest multiplicity events. Regarding the emission source shape, the correlation functions for both event sphericity classes show good agreement with an exponential shape, rather than a Gaussian one.

KEYWORDS: Heavy Ion Experiments, Particle correlations and fluctuations

ARXIV EPRINT: [1901.05518](https://arxiv.org/abs/1901.05518)

Contents

1	Introduction	1
2	Experimental setup and data selection	2
3	Analysis technique	3
3.1	Two-pion correlation function analysis	4
3.2	Systematic uncertainty	8
4	Results	8
5	Summary	10
	The ALICE collaboration	15

1 Introduction

Bose-Einstein correlations for pairs of identical bosons with low relative momentum are essential tools for understanding particle production in ultra-relativistic collision experiments [1–3]. They allow one to extract the dimensions of the freeze-out stage of the reaction, usually known as the “source radii”. A linear dependence of the volume defined by such radii on the charged-particle multiplicity produced in the event was observed in pp, p-Pb, and Pb-Pb collisions at the Large Hadron Collider (LHC) [4–10]. Interestingly, pp collisions at the LHC have reached multiplicities similar to the ones obtained in peripheral p-Pb and Pb-Pb collisions, thus allowing for a direct comparison of their source radii [7–9].

In proton-proton collisions, correlations of non-identical pions ($\pi^+\pi^-$) show significant deviations from unity particularly in low multiplicity events and at high pair transverse momentum $k_T = \frac{1}{2}|\mathbf{p}_1 + \mathbf{p}_2|_T$, which are attributed to resonance decays and fragmentation of mini-jets from low momentum-transfer scatterings [7, 8]. These correlations are a dominant background to the Bose-Einstein correlations between pairs of identical pions ($\pi^+\pi^+ + \pi^-\pi^-$) and make interferometry analyses at the LHC challenging for k_T greater than about 0.6 GeV/ c . However, the three-pion cumulant approach significantly suppresses the mini-jet related backgrounds in pp and p-Pb collisions [9], though it can suffer from statistical limitations.

In this paper, we introduce a new way of reducing the mini-jet background in pp collisions by selecting events based on their transverse sphericity [11, 12], an observable that is sensitive to particle collimation and as such can differentiate between jet-like (hard) and spherical (soft) event topologies. Such a differential measurement based on sphericity, k_T , and multiplicity, will offer new insights into (mini-jet induced) background correlations and offer invaluable information needed to improve the accuracy of event generators, such

as PYTHIA [13, 14]. As will be shown, this advancement can significantly extend the k_T reach of interferometry analyses in general.

This paper presents two-particle correlation functions (CFs) as a function of the pair relative three-momentum $q = \sqrt{(p_1 - p_2)^i (p_1 - p_2)_i}$ and the source radius parameter for different intervals of $dN_{\text{ch}}/d\eta$ and k_T for jet-like and spherical event topologies. In particular, the k_T dependence of the radii in spherical events is investigated since small background correlations in these events allows for the study of possible signs of collectivity in pp collisions.

2 Experimental setup and data selection

Approximately 5×10^8 pp collisions at $\sqrt{s} = 7$ TeV were analyzed, which were recorded by the ALICE experiment at the LHC [15, 16] during the 2010 running period.

The main detectors used for this analysis are: the Inner Tracking System (ITS) [17], the Time Projection Chamber (TPC) [18], the Time-Of-Flight detector (TOF) [19], and the V0 [20]. The ITS is a six-layer cylindrical silicon detector used for precise vertex and track reconstruction close to the interaction point. It provides full azimuthal coverage and spans the pseudorapidity range $|\eta| < 0.9$. The TPC is the main tracking detector in ALICE and measures the specific ionization energy loss of particles in the TPC gas for particle identification (PID). It covers the whole azimuth and provides a radial coverage of 159 possible space points for tracks. It fully covers the $|\eta| < 0.9$ range while extending out to $|\eta| < 1.5$ with a smaller number of potentially reconstructed space points. The TOF uses multigap resistive plate chambers to measure particle arrival time and thus particle velocity. It extends the PID capabilities to the intermediate p_T range where the pion, proton, and kaon energy loss signals are similar in the TPC. The V0 detectors are used for triggering on collision events. They are composed of two small-angle scintillator arrays, located at 340 cm and -90 cm from the nominal interaction point along the beam line. The minimum-bias trigger, which is used in this analysis, requires at least one hit in the V0 or either of the two first layers of the ITS in coincidence with two beam bunches crossing in the ALICE interaction region, which is measured by a beam-pickup system. An offline event selection is applied to reject beam-halo induced events and beam-gas collisions.

Accepted events have their primary vertex reconstructed within ± 8 cm from the center of the detector along the beam line in order to ensure uniform tracking performance. Charged particle tracks are reconstructed with the ITS and TPC detectors, requiring that each TPC track segment is reconstructed from at least 70 out of the 159 possible space points. To guarantee that mainly primary particles are selected it is required that the track has its Distance of Closest Approach (DCA) to the primary vertex smaller than $(0.0182 + 0.35 \cdot p_T^{-1.01})$ cm in the transverse plane, with p_T in GeV/ c , and 0.2 cm in the longitudinal direction. Tracks with a kink topology in the TPC, indicating weak decays of charged kaons, are rejected. Two-track effects such as merging and splitting are minimized using pion pair selection criteria as described in [7] and are known to be negligible in this p_T range for q greater than about 50 MeV/ c , which is much less than the expected width of the Bose-Einstein correlation peak.

$N_{\text{ch}}^{\text{rec}}$	$\langle dN_{\text{ch}}/d\eta \rangle_{S_{\text{T}} < 0.3}$	$\langle dN_{\text{ch}}/d\eta \rangle_{S_{\text{T}} > 0.7}$
[1,13]	4.3 ± 2.0	5.3 ± 2.2
[14,21]	9.6 ± 2.0	10.5 ± 2.1
[22,30]	13.9 ± 2.2	14.9 ± 2.3
[31,54]	18.7 ± 3.2	20.4 ± 3.2

Table 1. Intervals of $N_{\text{ch}}^{\text{rec}}$ and corresponding mid-rapidity $\langle dN_{\text{ch}}/d\eta \rangle$ with $|\eta| < 1.2$ and $0.13 < p_{\text{T}} < 4.0 \text{ GeV}/c$ for both sphericity ranges.

3 Analysis technique

The interferometry analysis was performed using pions with pseudorapidity $|\eta| < 1.2$ and transverse momentum $0.13 < p_{\text{T}} < 4.0 \text{ GeV}/c$. Pions were identified by their specific ionization energy loss in the TPC as well as the measured pion arrival time in the TOF detector. The PID selection criteria are the same as described in [7]. They are optimized to maximize efficiency while producing a high-purity of the pion sample of about 99% for $p_{\text{T}} < 2.5 \text{ GeV}/c$. The p_{T} resolution is about 1% or better in the relevant p_{T} range.

Transverse sphericity is calculated by using all charged tracks with $|\eta| < 0.8$ and $p_{\text{T}} > 0.5 \text{ GeV}/c$. In order to avoid a bias from the boost along the beam axis [12], the event shape is calculated only in the transverse plane. The transverse sphericity matrix S_{XY} is defined as

$$S_{\text{XY}} = \frac{1}{\sum_i p_{\text{T}}^i} \sum_i \frac{1}{p_{\text{T}}^i} \begin{pmatrix} (p_x^i)^2 & p_x^i \cdot p_y^i \\ p_x^i \cdot p_y^i & (p_y^i)^2 \end{pmatrix}, \quad (3.1)$$

where i runs over all charged particle tracks in the event. By using the transverse sphericity matrix eigenvalues λ_1 and λ_2 [11], the transverse sphericity is computed as

$$S_{\text{T}} = \frac{2 \cdot \min(\lambda_1, \lambda_2)}{\lambda_1 + \lambda_2}. \quad (3.2)$$

It is a bounded scalar observable that is sensitive to the event shape, and in particular particle collimation. An event with only one hard scattering will in general produce a jet-like distribution that yields low sphericity while multiple soft scatterings are expected to yield high sphericity events. Events with several independent hard scatterings can also yield higher sphericity as each (mini-)jet axis is oriented randomly. Transverse sphericity is known to be correlated with the number of hard parton-parton interactions in an event [11]. In this work jet-like events with $S_{\text{T}} < 0.3$ and spherical events with $S_{\text{T}} > 0.7$ are analyzed, which comprise 18% and 28% of the total minimum-bias data set, respectively.

The resolution in S_{T} due to finite track reconstruction efficiency is found to be better than 0.1 based on Monte-Carlo (MC) simulations with the PYTHIA 6.4 Perugia-0 tune [13, 14], for both low- and high-sphericity events in any multiplicity interval. No significant effect from the finite track momentum resolution was observed in simulations.

The multiplicity estimator $N_{\text{ch}}^{\text{rec}}$ is defined as the number of reconstructed charged-particle tracks that enter the interferometry analysis. The intervals and their corresponding corrected $\langle dN_{\text{ch}}/d\eta \rangle$ for both sphericity selections are shown in table 1.

3.1 Two-pion correlation function analysis

The one-dimensional femtoscopic analysis presented in this paper was performed using the invariant momentum difference q , which corresponds to the magnitude of the relative three-momentum in the pair rest frame (PRF). The measured CFs are defined as the ratio of the q distributions for same-event (A) and mixed-event (B) pion pairs times a normalization factor (ξ) [3],

$$C(q; N_{\text{ch}}^{\text{rec}}, S_{\text{T}}) = \xi(N_{\text{ch}}^{\text{rec}}, S_{\text{T}}) \cdot \frac{A(q; N_{\text{ch}}^{\text{rec}}, S_{\text{T}})}{B(q; N_{\text{ch}}^{\text{rec}}, S_{\text{T}})}. \quad (3.3)$$

For the event mixing, pools of eight events of similar multiplicity and sphericity are formed. In addition, it is also required that events in a mixed event pool have their vertex positions within 2 cm from each other in the beam direction. The mixed event distributions were then made by pairing up pions from different events in a mixed event pool. Identical selection criteria are applied to the same-event and mixed-event pion pairs, and both $A(q)$ and $B(q)$ are constructed in the same S_{T} interval.

Both distributions are normalized in the range $0.7 < q < 0.8 \text{ GeV}/c$, which is well outside the relevant quantum statistical (QS) domain ($q \propto 1/R \approx 0.3 \text{ GeV}/c$) and below the onset of the high- q rise associated with energy and momentum conservation.

Figure 1 shows good agreement between the measured correlation functions for opposite-sign pion pairs in pp collisions at $\sqrt{s} = 7 \text{ TeV}$ and PYTHIA simulations, which include the ALICE detector response, for spherical and jet-like events at similar multiplicity. Opposite-sign CFs do not include Bose-Einstein correlations but do include backgrounds, such as those induced by mini-jets, which are also found in same-sign pair analyses [7]. They also show features due to two-body decays like K_{S}^0 and $\rho \rightarrow \pi^+\pi^-$ at about 412 and 723 MeV/ c in q respectively, and a wide three-body decay peak from $\omega \rightarrow \pi^+\pi^-\pi^0$.

The $C(q)$ in spherical events are relatively flat at unity, while the low S_{T} CFs exhibit a very pronounced slope. This finding supports previous assumptions about the mini-jet origin of background correlations in interferometry analyses [7] and demonstrates that PYTHIA describes two-pion correlations well in the absence of Bose-Einstein correlations.

Figure 2 shows a comparison of CFs for same-sign pion pairs from data and PYTHIA simulations for the two sphericity intervals at similar reconstructed multiplicity. The MC includes neither quantum-statistical correlations nor final-state interactions (FSI).

Similar to the opposite-sign CF at $S_{\text{T}} > 0.7$ shown in figure 1, the spherical-event same-sign CF is rather flat outside the QS correlation region ($q < 0.5 \text{ GeV}/c$). This indicates that the background is small in spherical events for same-sign pairs. The shape of the same-sign $C(q)$ in spherical events is compatible with the expectation from Bose-Einstein correlations. There are no novel features like peaks or depressions and the correlation function does not extend outside the theoretically predicted values $1 \leq C(q) \leq 2$. On the other hand, for jet-like events, the CF exhibits a pronounced slope over the full q range, indicating the presence of background. The CF shape is well described by PYTHIA outside the QS correlation region. Moreover, it is observed that the large- q correlation increases with k_{T} and decreases with multiplicity, which is consistent with previous findings in [7]. These results suggest that the primary source of background correlations in two-pion femtoscopic

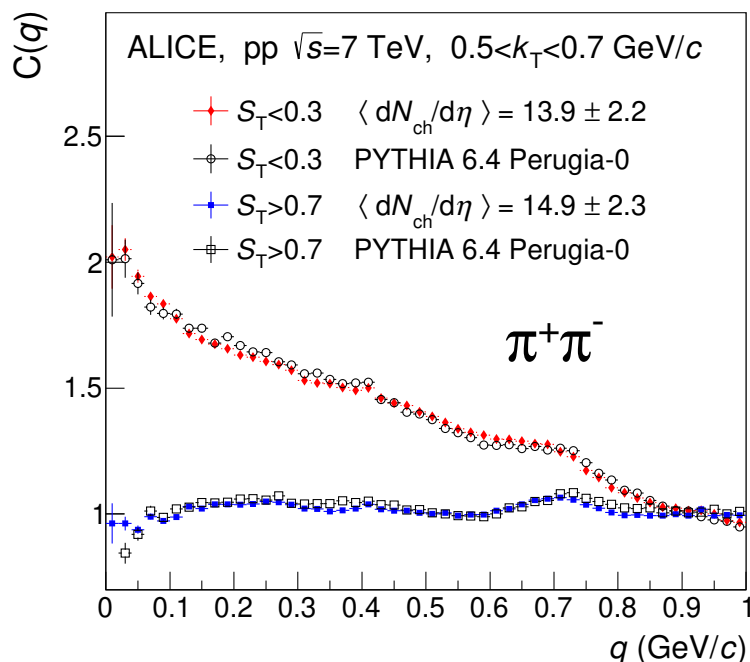


Figure 1. Opposite-sign pion pair correlation functions in data and PYTHIA simulations for high and low sphericity intervals. The error bars represent statistical uncertainties.

analyses is related to semi-hard scattering processes which predominantly populate jet-like event topologies.

To extract the source size from the measured correlation functions, background correlations are corrected with simulated CFs ($C_{MC}(q)$). This procedure assumes that the signal and background factorize and was used in a similar way by other experiments [4, 10]. The method also resembles [21] where the background signal is not extracted from MC simulations but fitted in the measured opposite-sign correlations and then removed out via the fitting procedure in the same-sign analysis. In the case of our analysis this approach showed to be unstable.

The simulations used for the corrections include the ALICE detector response and are analyzed exactly the same as the data. The corrected correlation function $\tilde{C}(q)$ can then be expressed as

$$\tilde{C}(q) = \frac{C_{\text{data}}(q)}{C_{MC}(q)} = \frac{C_{\text{BE+FSI}}(q) \cdot C_{\text{ES}}(q)}{C_{\text{ES}}^{MC}(q)}, \quad (3.4)$$

where $C_{\text{BE+FSI}}$ and C_{ES} are contributions coming from Bose-Einstein correlations with FSI effects and event shape dependent backgrounds, respectively. The corrected CFs, $\tilde{C}(q)$, are obtained separately for spherical and jet-like events. The femtoscopic correlations are then determined using

$$\tilde{C}(q) = [(1 - f_c^2) + f_c^2 K(q) C^{\text{QS}}(q)], \quad (3.5)$$

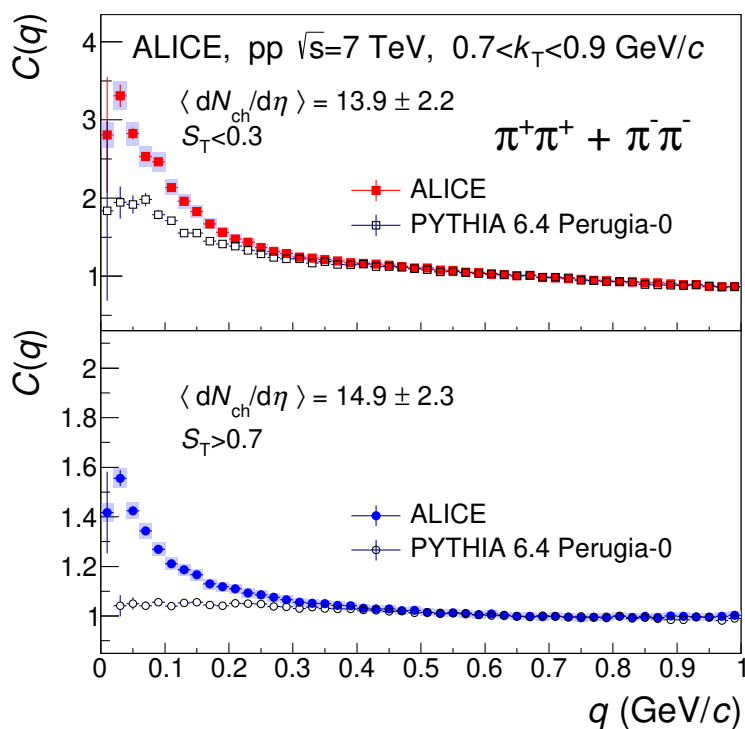


Figure 2. Comparison of same-sign correlation functions for data and PYTHIA simulations for both sphericity intervals. The error bars represent statistical uncertainties and the shaded boxes are systematic uncertainties. Note that the vertical axes have different scales in the two panels.

as in [22], where f_c^2 is the pair fraction from the core of the particle-emission source [23], $K(q)$ is the FSI correlation and $C^{QS}(q)$ is the extracted QS correlation. The $K(q)$ factor is well known and calculated using the two-pion FSI wave functions [24] that include Coulomb and strong interactions. The values of f_c^2 are estimated from EPOS-LHC MC model [25], which is known to reproduce a variety of LHC measurements. The deviation of f_c^2 from unity quantifies the degree of dilution caused by pions from long-lived resonances and weak decays. This effect is suppressed by the track selection used. In previous measurements [9], f_c^2 showed little dependence on k_T up to $0.7 \text{ GeV}/c$ and calculations using EPOS-LHC agreed with this observation at even larger values of k_T . At all k_T , the final value of f_c^2 depended on the track selection, leading to larger values of f_c^2 in cases where a tighter DCA selection was used [26]. In this analysis, the f_c^2 is fixed to 0.85 which corresponds to its k_T -averaged value. Finally, a fit is applied to the extracted $C^{QS}(q)$ correlations in order to determine the femtoscopic radii.

In past analyses [27], it was observed that a Gaussian form of $C^{QS}(q)$ does not describe the observed one-dimensional CFs over the full q range. Previous analyses at the LHC showed that this remains the case at much higher collision energy [4, 5]. Hence, a Levy fit is performed, employing a free parameter α in the exponent, where $\alpha = 2$ corresponds to a Gaussian distribution. Figure 3 shows the fits of $C^{QS}(q)$ with Gaussian

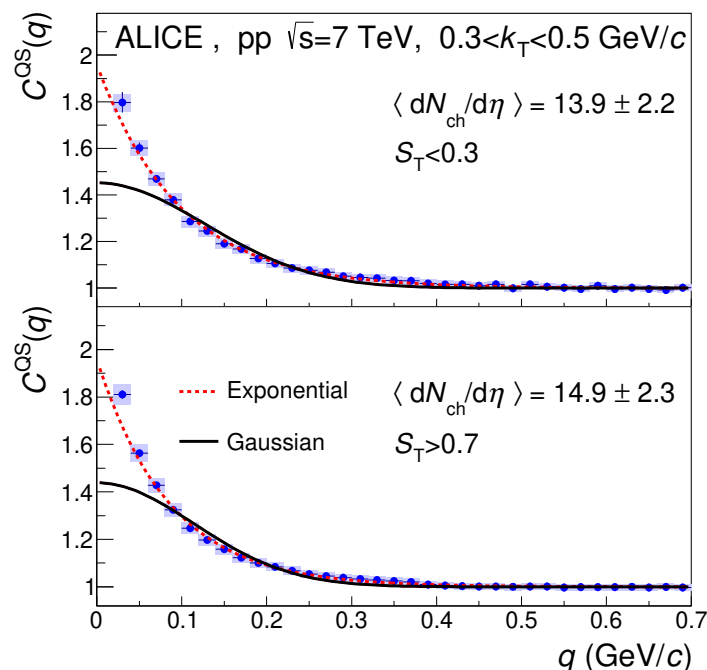


Figure 3. Comparison of exponential and Gaussian fit results for $C^{QS}(q)$ functions in spherical and jet-like events.

and exponential functional forms, and it is observed that the 1D CFs are better described by $\alpha = 1$ corresponding to an exponential distribution. Therefore, femtoscopic radii are extracted assuming an exponential shape:

$$C^{QS}(q) = 1 + \lambda \cdot e^{(-R_{inv} \cdot q)}. \quad (3.6)$$

In the fitting procedure, λ was first treated as a fit parameter and showed negligible k_T dependence. The mean value of λ was then obtained for each sphericity interval and fixed for the final fitting. Since the expected dilution from long-lived resonance decays and weak decays is explicitly removed in eq. 3.5, the λ parameter is expected to be consistent with unity in the case of fully chaotic emission and exponential 1D correlation functions. At $k_T < 0.7 \text{ GeV}/c$, the mean value of λ is 0.97 for spherical and 1.0 for jet-like events, with small deviations consistent with statistical fluctuation in each individual measurement.

To extract radii the correlation functions are fit with the same functional form for each k_T interval while fixing λ to the aforementioned mean values. No additional normalization factors are used in fitting $C^{QS}(q)$.

A previous sphericity-integrated measurement [10], using a significantly different fitting procedure and thus having an alternative interpretation of the λ parameter to the one used in this paper, observed a stronger k_T dependence of both the radii and λ parameters. Considering the different parameterizations used in [26], model calculations and previous measurements [26], it is unlikely that there exists such a significant change in the fraction of long-lived emitters or pion coherence to explain such a strong decrease of λ with k_T .

3.2 Systematic uncertainty

Analyses were performed using data from different data-taking periods with varying experimental conditions (e.g. detector operating conditions, polarity of the magnetic field in the apparatus, etc.) and showed negligible differences in the observed radii. Similarly, a 100% increase in the number of events that are used in the mixing procedure also produced negligible differences in the measured radii. Separate analyses for positively and negatively charged pions, which, at LHC energies, are expected to give identical results, gave less than 0.2% differences in measured radii.

Regarding more substantial uncertainties in the measured radii a distinction was made between point-by-point uncorrelated and correlated sources of systematic uncertainty. It was observed that there are two significant sources of uncorrelated systematic uncertainty, the first one being variations in the tracking procedure, and the second one being variations in the CF fit range. The uncorrelated uncertainty due to the tracking procedure is evaluated by using an alternative track selection for the analysis, in which only the TPC is used to reconstruct tracks as in [7], and is estimated to be up to 10% on the measured radii. Concerning the uncertainty due to the fit range selection, in this analysis $q < 0.7 \text{ GeV}/c$ was used as the default fit range while $q < 0.4 \text{ GeV}/c$ and $q < 1.0 \text{ GeV}/c$ were the variations. A difference in radii of up to 5% is observed in this case with the smaller fit range always having a larger influence on the change of radii, as is expected.

In this analysis, the correlated uncertainties in the measured radii are shown to be larger than the uncorrelated ones and are estimated by varying f_c^2 , sphericity ranges and Monte Carlo generators. A variation in f_c^2 of ± 0.05 produced a 5–10% uncertainty, with the largest deviation being observed in the highest N_{ch} and k_T bin. The variation of the sphericity range, which was varied by ± 0.05 , contributed up to 10% in the systematic uncertainty. The leading source of correlated uncertainty, which shows a difference in the radii of up to 15% depending on the k_T and multiplicity bin, is the choice of Monte Carlo generators for the background correlations. In this analysis we used PYTHIA as the default and PHOJET [28] as the variation. As is expected, the spherical event results are less effected by this variation than the jet-like event ones.

4 Results

Figure 4 shows the measured R_{inv} as a function of pair k_T for spherical and jet-like events in different multiplicity intervals. In comparison to previously observed 1D radii [7], the multiplicity- and k_T -dependence observed in the event shape dependent analysis show both similarities and significant differences depending on the sphericity selection. In spherical events the dependence of the radii on k_T is well described by a constant. As is expected, the fitted constant radius increases with multiplicity from $1.971 \pm 0.006 \text{ (stat.)} \pm 0.106 \text{ (sys.) fm}$ in the lowest multiplicity bin to $2.410 \pm 0.007 \text{ (stat.)} \pm 0.050 \text{ (sys.) fm}$ at the highest multiplicity. On the other hand, similar to previous sphericity-integrated results, the jet-like radius dependence on k_T is not well described by a 0th-order polynomial (χ^2/N_{dof} is larger than 10), however a 1st-order polynomial does manage to describe the data better. The constant of this fit is $1.97 \pm 0.01 \text{ (stat.)} \pm 0.11 \text{ (sys.) fm}$ at lowest multiplicity and increases

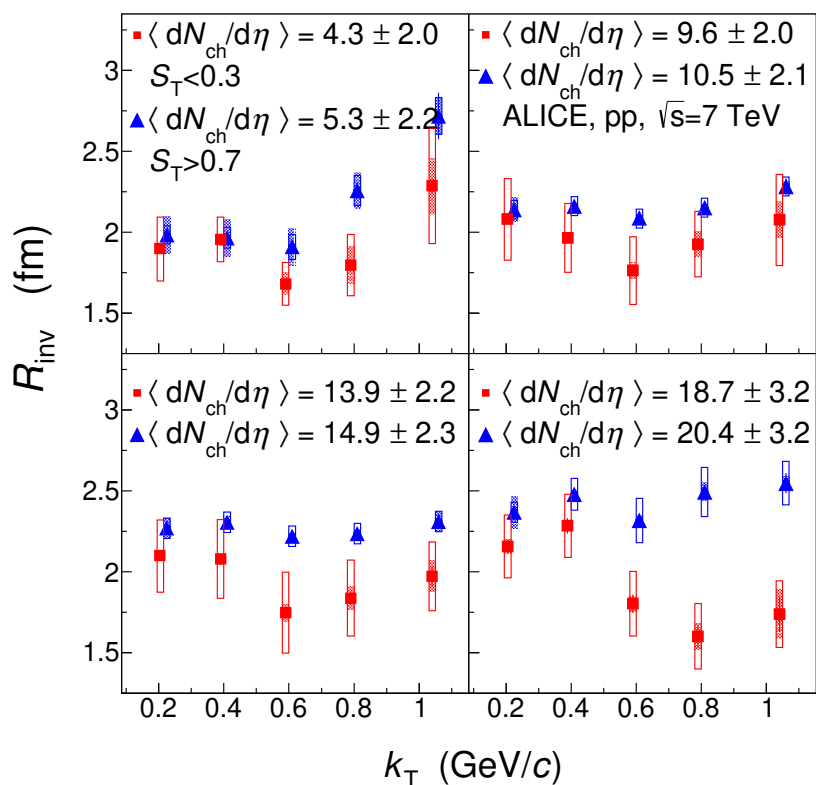


Figure 4. Measured 1D source radii as a function of pair k_T for spherical and jet-like events in pp collisions at $\sqrt{s} = 7$ TeV. Points are shifted horizontally for clarity. The vertical error bars represent the statistical uncertainties of the measurement, while the shaded and open boxes represent the uncorrelated and correlated systematic uncertainties, respectively.

to 2.40 ± 0.05 (stat.) ± 0.05 (sys.) fm at highest multiplicity. The slope parameter is observed to be negative except for the lowest multiplicity bin where it is consistent with zero. For higher multiplicities the difference from a zero slope is observed as a 3σ , 7.3σ and 4.1σ effect consecutively.

In spherical events the overall size of the system grows with increasing event multiplicity. Such a trend has been observed in all previous measurements in proton-proton and heavy-ion collisions. Spherical events are expected to contain multiple scatterings, so a growth of system size with multiplicity is naturally expected. On the other hand, jet-like events are typically dominated by a single interaction with a large momentum transfer and subsequent fragmentation into (mini-)jets where most of particle production occurs.

Our data suggest that the hard scattering process has a non-trivial space-time structure which is consistent with some theoretical predictions [29]. It is not possible to provide a more direct interpretation of the results, because the modeling of the space-time structure of the fragmentation process is largely neglected in current Monte-Carlo codes such as PYTHIA and PHOJET.

The k_T dependence of R_{inv} in jet-like events is much less explored theoretically, due to the reasons given above. Therefore, our measurements present a pioneering insight into the space-time characteristics of fragmentation. It is observed that for higher multiplicity ranges the k_T dependence has a non-zero slope, for example -0.52 ± 0.05 (stat.) ± 0.05 (sys.) fm/(GeV/ c) for the second highest multiplicity selection, obtained from a linear fit to the radii, taking into account all sources of systematic uncertainties. These results raise an interesting question on the origin of the k_T dependence in minimum bias 1D measurements by ALICE [7], especially if considered together with the lack of such a decrease in spherical events. It is confirmed that by averaging the radii from spherical, jet-like and intermediate events ($0.3 < S_T < 0.7$, not shown in this work) it is possible to reproduce the dependence observed in the sphericity-integrated analysis. The fact that in a differential measurement the slope is most prominent in jet-like events suggests that it is this category of events that might be the dominant source of the non-zero k_T slope in the minimum-bias data set as well.

The development of a Monte-Carlo code that fully incorporates the space-time structure of proton-proton collisions and the fragmentation process would be highly desirable, a candidate for such an event generator would be EPOS [25]. The predictions of such a model, as a function of event sphericity, should then be carefully compared with existing and future data on pion Bose-Einstein correlations. Further improvements in the modeling of experimental transverse sphericity distributions is also desirable.

In a three-dimensional analysis of femtoscopic radii in the Longitudinally Co-Moving System (LCMS), which is the reference system where pair longitudinal momentum vanishes, with the Pratt-Bertsch decomposition of the momentum difference, where the “long” direction is along the beam, “out” is along pair transverse momentum and “side” is perpendicular to the other two, a decreasing trend with k_T is interpreted as evidence of hydrodynamic collectivity [30]. This reasoning has also been applied to small systems [25], therefore this dependence is a critical test of the interpretation of spherical and jet-like events presented above. However, it was shown that the k_T dependence in the PRF is additionally influenced by the boost factor between the LCMS and the PRF [31, 32]. Therefore, in this work we are not able to draw conclusions about collectivity in pp collisions based on the k_T dependence observed in figure 4.

5 Summary

In summary, the measured pp collisions at $\sqrt{s} = 7$ TeV have been classified into sub-samples with high (“spherical”) and low (“jet-like”) sphericity and source radii have been extracted for both. An exponential fit function, as opposed to a Gaussian, was shown to better describe the observed 1D correlation functions for both sphericity ranges. A significant suppression of non-femtoscopic correlations was observed in “spherical” events, effectively doubling the k_T range of femtoscopic analyses for this sample. Substantial background correlations remained in the “jet-like” sample, which is consistent with the hypothesis that the main source of these correlations is mini-jets. PYTHIA and PHOJET describe this background, making an effective background removal procedure feasible. As a consequence,

radii for jet-like events have been extracted for the first time. They tend to be smaller in comparison to source radii of spherical events, which may be a consequence of lower average multiplicities, and show a decrease with k_T , resembling the trend observed also in minimum-bias analyses. The extracted radii in spherical events show an increase in the system size with multiplicity, in agreement with previous measurements and model expectations. They are also observed to have a flat trend in k_T , which differs from the k_T dependence that was previously observed in 1D minimum-bias analyses [4–10]. This suggests that the observed slope in minimum-bias events could be arising from the lower part of the transverse sphericity spectrum in pp collisions. This is novel and unique information on the space-time characteristics of the fragmentation process. Future investigations will require more advanced modeling of the space-time properties of particle production in Monte-Carlo codes, and a comparison of such theoretical predictions to a three-dimensional pion femtoscopy measurement performed differentially in transverse sphericity.

Acknowledgments

The ALICE Collaboration would like to thank all its engineers and technicians for their invaluable contributions to the construction of the experiment and the CERN accelerator teams for the outstanding performance of the LHC complex. The ALICE Collaboration gratefully acknowledges the resources and support provided by all Grid centres and the Worldwide LHC Computing Grid (WLCG) collaboration. The ALICE Collaboration acknowledges the following funding agencies for their support in building and running the ALICE detector: A. I. Alikhanyan National Science Laboratory (Yerevan Physics Institute) Foundation (ANSL), State Committee of Science and World Federation of Scientists (WFS), Armenia; Austrian Academy of Sciences and Nationalstiftung für Forschung, Technologie und Entwicklung, Austria; Ministry of Communications and High Technologies, National Nuclear Research Center, Azerbaijan; Conselho Nacional de Desenvolvimento Científico e Tecnológico (CNPq), Universidade Federal do Rio Grande do Sul (UFRGS), Financiadora de Estudos e Projetos (Finep) and Fundação de Amparo à Pesquisa do Estado de São Paulo (FAPESP), Brazil; Ministry of Science & Technology of China (MSTC), National Natural Science Foundation of China (NSFC) and Ministry of Education of China (MOEC), China; Croatian Science Foundation and Ministry of Science and Education, Croatia; Centro de Aplicaciones Tecnológicas y Desarrollo Nuclear (CEADEN), Cubaenergía, Cuba; Ministry of Education, Youth and Sports of the Czech Republic, Czech Republic; The Danish Council for Independent Research — Natural Sciences, the Carlsberg Foundation and Danish National Research Foundation (DNRF), Denmark; Helsinki Institute of Physics (HIP), Finland; Commissariat à l’Energie Atomique (CEA) and Institut National de Physique Nucléaire et de Physique des Particules (IN2P3) and Centre National de la Recherche Scientifique (CNRS), France; Bundesministerium für Bildung, Wissenschaft, Forschung und Technologie (BMBF) and GSI Helmholtzzentrum für Schwerionenforschung GmbH, Germany; General Secretariat for Research and Technology, Ministry of Education, Research and Religions, Greece; National Research, Development and Innovation Office, Hungary; Department of Atomic Energy Government of India (DAE),

Department of Science and Technology, Government of India (DST), University Grants Commission, Government of India (UGC) and Council of Scientific and Industrial Research (CSIR), India; Indonesian Institute of Science, Indonesia; Centro Fermi — Museo Storico della Fisica e Centro Studi e Ricerche Enrico Fermi and Istituto Nazionale di Fisica Nucleare (INFN), Italy; Institute for Innovative Science and Technology, Nagasaki Institute of Applied Science (IIST), Japan Society for the Promotion of Science (JSPS) KAKENHI and Japanese Ministry of Education, Culture, Sports, Science and Technology (MEXT), Japan; Consejo Nacional de Ciencia (CONACYT) y Tecnología, through Fondo de Cooperación Internacional en Ciencia y Tecnología (FONCICYT) and Dirección General de Asuntos del Personal Académico (DGAPA), Mexico; Nederlandse Organisatie voor Wetenschappelijk Onderzoek (NWO), Netherlands; The Research Council of Norway, Norway; Commission on Science and Technology for Sustainable Development in the South (COMSATS), Pakistan; Pontificia Universidad Católica del Perú, Peru; Ministry of Science and Higher Education and National Science Centre, Poland; Korea Institute of Science and Technology Information and National Research Foundation of Korea (NRF), Republic of Korea; Ministry of Education and Scientific Research, Institute of Atomic Physics and Romanian National Agency for Science, Technology and Innovation, Romania; Joint Institute for Nuclear Research (JINR), Ministry of Education and Science of the Russian Federation, National Research Centre Kurchatov Institute, Russian Science Foundation and Russian Foundation for Basic Research, Russia; Ministry of Education, Science, Research and Sport of the Slovak Republic, Slovakia; National Research Foundation of South Africa, South Africa; Swedish Research Council (VR) and Knut & Alice Wallenberg Foundation (KAW), Sweden; European Organization for Nuclear Research, Switzerland; National Science and Technology Development Agency (NSDTA), Suranaree University of Technology (SUT) and Office of the Higher Education Commission under NRU project of Thailand, Thailand; Turkish Atomic Energy Agency (TAEK), Turkey; National Academy of Sciences of Ukraine, Ukraine; Science and Technology Facilities Council (STFC), United Kingdom; National Science Foundation of the United States of America (NSF) and United States Department of Energy, Office of Nuclear Physics (DOE NP), United States of America.

Open Access. This article is distributed under the terms of the Creative Commons Attribution License ([CC-BY 4.0](https://creativecommons.org/licenses/by/4.0/)), which permits any use, distribution and reproduction in any medium, provided the original author(s) and source are credited.

References

- [1] U.W. Heinz and B.V. Jacak, *Two particle correlations in relativistic heavy ion collisions*, *Ann. Rev. Nucl. Part. Sci.* **49** (1999) 529 [[nucl-th/9902020](#)] [[INSPIRE](#)].
- [2] U.A. Wiedemann and U.W. Heinz, *Particle interferometry for relativistic heavy ion collisions*, *Phys. Rept.* **319** (1999) 145 [[nucl-th/9901094](#)] [[INSPIRE](#)].
- [3] M.A. Lisa, S. Pratt, R. Soltz and U. Wiedemann, *Femtoscopia in relativistic heavy ion collisions*, *Ann. Rev. Nucl. Part. Sci.* **55** (2005) 357 [[nucl-ex/0505014](#)] [[INSPIRE](#)].

- [4] CMS collaboration, *First measurement of Bose-Einstein correlations in proton-proton collisions at $\sqrt{s} = 0.9$ and 2.36 TeV at the LHC*, *Phys. Rev. Lett.* **105** (2010) 032001 [[arXiv:1005.3294](#)] [[INSPIRE](#)].
- [5] ALICE collaboration, *Two-pion Bose-Einstein correlations in pp collisions at $\sqrt{s} = 900$ GeV*, *Phys. Rev. D* **82** (2010) 052001 [[arXiv:1007.0516](#)] [[INSPIRE](#)].
- [6] CMS collaboration, *Measurement of Bose-Einstein correlations in pp collisions at $\sqrt{s} = 0.9$ and 7 TeV*, *JHEP* **05** (2011) 029 [[arXiv:1101.3518](#)] [[INSPIRE](#)].
- [7] ALICE collaboration, *Femtoscopy of pp collisions at $\sqrt{s} = 0.9$ and 7 TeV at the LHC with two-pion Bose-Einstein correlations*, *Phys. Rev. D* **84** (2011) 112004 [[arXiv:1101.3665](#)] [[INSPIRE](#)].
- [8] ALICE collaboration, *Two-pion femtoscopy in p-Pb collisions at $\sqrt{s_{NN}} = 5.02$ TeV*, *Phys. Rev. C* **91** (2015) 034906 [[arXiv:1502.00559](#)] [[INSPIRE](#)].
- [9] ALICE collaboration, *Freeze-out radii extracted from three-pion cumulants in pp, p-Pb and Pb-Pb collisions at the LHC*, *Phys. Lett. B* **739** (2014) 139 [[arXiv:1404.1194](#)] [[INSPIRE](#)].
- [10] ATLAS collaboration, *Two-particle Bose-Einstein correlations in pp collisions at $\sqrt{s} = 0.9$ and 7 TeV measured with the ATLAS detector*, *Eur. Phys. J. C* **75** (2015) 466 [[arXiv:1502.07947](#)] [[INSPIRE](#)].
- [11] ALICE collaboration, *Transverse sphericity of primary charged particles in minimum bias proton-proton collisions at $\sqrt{s} = 0.9, 2.76$ and 7 TeV*, *Eur. Phys. J. C* **72** (2012) 2124 [[arXiv:1205.3963](#)] [[INSPIRE](#)].
- [12] A. Banfi, G.P. Salam and G. Zanderighi, *Resummed event shapes at hadron-hadron colliders*, *JHEP* **08** (2004) 062 [[hep-ph/0407287](#)] [[INSPIRE](#)].
- [13] T. Sjöstrand, S. Mrenna and P.Z. Skands, *PYTHIA 6.4 physics and manual*, *JHEP* **05** (2006) 026 [[hep-ph/0603175](#)] [[INSPIRE](#)].
- [14] P.Z. Skands, *Tuning Monte Carlo generators: the Perugia tunes*, *Phys. Rev. D* **82** (2010) 074018 [[arXiv:1005.3457](#)] [[INSPIRE](#)].
- [15] ALICE collaboration, *The ALICE experiment at the CERN LHC*, 2008 *JINST* **3** S08002 [[INSPIRE](#)].
- [16] ALICE collaboration, *Performance of the ALICE experiment at the CERN LHC*, *Int. J. Mod. Phys. A* **29** (2014) 1430044 [[arXiv:1402.4476](#)] [[INSPIRE](#)].
- [17] ALICE collaboration, *Alignment of the ALICE inner tracking system with cosmic-ray tracks*, 2010 *JINST* **5** P03003 [[arXiv:1001.0502](#)] [[INSPIRE](#)].
- [18] J. Alme et al., *The ALICE TPC, a large 3-dimensional tracking device with fast readout for ultra-high multiplicity events*, *Nucl. Instrum. Meth. A* **622** (2010) 316 [[arXiv:1001.1950](#)] [[INSPIRE](#)].
- [19] ALICE collaboration, *ALICE Time-Of Flight system (TOF): addendum to the technical design report*, CERN-LHCC-2002-016, CERN, Geneva, Switzerland (2002).
- [20] ALICE collaboration, *Performance of the ALICE VZERO system*, 2013 *JINST* **8** P10016 [[arXiv:1306.3130](#)] [[INSPIRE](#)].
- [21] CMS collaboration, *Bose-Einstein correlations in pp, pPb and PbPb collisions at $\sqrt{s_{NN}} = 0.9-7$ TeV*, *Phys. Rev. C* **97** (2018) 064912 [[arXiv:1712.07198](#)] [[INSPIRE](#)].

- [22] Yu. Sinyukov, R. Lednicky, S.V. Akkelin, J. Pluta and B. Erazmus, *Coulomb corrections for interferometry analysis of expanding hadron systems*, *Phys. Lett. B* **432** (1998) 248 [[INSPIRE](#)].
- [23] T. Csorgo, B. Lorstad, J. Schmid-Sorensen and A. Ster, *Partial coherence in the core/halo picture of Bose-Einstein n particle correlations*, *Eur. Phys. J. C* **9** (1999) 275 [[hep-ph/9812422](#)] [[INSPIRE](#)].
- [24] R. Lednicky, *Finite-size effects on two-particle production in continuous and discrete spectrum*, *Phys. Part. Nucl.* **40** (2009) 307 [[nucl-th/0501065](#)] [[INSPIRE](#)].
- [25] T. Pierog, I. Karpenko, J.M. Katzy, E. Yatsenko and K. Werner, *EPOS LHC: test of collective hadronization with data measured at the CERN Large Hadron Collider*, *Phys. Rev. C* **92** (2015) 034906 [[arXiv:1306.0121](#)] [[INSPIRE](#)].
- [26] ALICE collaboration, *Two- and three-pion quantum statistics correlations in Pb-Pb collisions at $\sqrt{s_{NN}} = 2.76$ TeV at the CERN Large Hadron Collider*, *Phys. Rev. C* **89** (2014) 024911 [[arXiv:1310.7808](#)] [[INSPIRE](#)].
- [27] A. Bialas, M. Kucharczyk, H. Palka and K. Zalewski, *Mass dependence of HBT correlations in e^+e^- annihilation*, *Phys. Rev. D* **62** (2000) 114007 [[hep-ph/0006290](#)] [[INSPIRE](#)].
- [28] R. Engel, *Photoproduction within the two component dual parton model 1. Amplitudes and cross-sections*, *Z. Phys. C* **66** (1995) 203 [[INSPIRE](#)].
- [29] G. Paic and P.K. Skowronski, *Effect of hard processes on momentum correlations in pp and $p\bar{p}$ collisions*, *J. Phys. G* **31** (2005) 1045 [[hep-ph/0504051](#)] [[INSPIRE](#)].
- [30] ALICE collaboration, *Centrality dependence of pion freeze-out radii in Pb-Pb collisions at $\sqrt{s_{NN}} = 2.76$ TeV*, *Phys. Rev. C* **93** (2016) 024905 [[arXiv:1507.06842](#)] [[INSPIRE](#)].
- [31] V.M. Shapoval, P. Braun-Munzinger, I.A. Karpenko and Yu.M. Sinyukov, *Femtoscopic scales in pp and pPb collisions in view of the uncertainty principle*, *Phys. Lett. B* **725** (2013) 139 [[arXiv:1304.3815](#)] [[INSPIRE](#)].
- [32] A. Kisiel, M. Gałażyn and P. Bożek, *Pion, kaon and proton femtoscopy in Pb-Pb collisions at $\sqrt{s_{NN}} = 2.76$ TeV modeled in $(3+1)D$ hydrodynamics*, *Phys. Rev. C* **90** (2014) 064914 [[arXiv:1409.4571](#)] [[INSPIRE](#)].

The ALICE collaboration

S. Acharya¹⁴⁰, D. Adamová⁹³, S.P. Adhya¹⁴⁰, A. Adler⁷⁴, J. Adolfsson⁸⁰, M.M. Aggarwal⁹⁸, G. Aglieri Rinella³⁴, M. Agnello³¹, N. Agrawal⁴⁸, Z. Ahammed¹⁴⁰, S. Ahmad¹⁷, S.U. Ahn⁷⁶, S. Aiola¹⁴⁵, A. Akindinov⁶⁴, M. Al-Turany¹⁰⁴, S.N. Alam¹⁴⁰, D.S.D. Albuquerque¹²¹, D. Aleksandrov⁸⁷, B. Alessandro⁵⁸, H.M. Alfanda⁶, R. Alfaro Molina⁷², Y. Ali¹⁵, A. Alici^{10,27,53}, A. Alkin², J. Alme²², T. Alt⁶⁹, L. Altenkamper²², I. Altsybeev¹¹¹, M.N. Anaam⁶, C. Andrei⁴⁷, D. Andreou³⁴, H.A. Andrews¹⁰⁸, A. Andronic^{143,104}, M. Angeletti³⁴, V. Anguelov¹⁰², C. Anson¹⁶, T. Antičić¹⁰⁵, F. Antinori⁵⁶, P. Antonioli⁵³, R. Anwar¹²⁵, N. Apadula⁷⁹, L. Aphecetche¹¹³, H. Appelshäuser⁶⁹, S. Arcelli²⁷, R. Arnaldi⁵⁸, I.C. Arsene²¹, M. Arslanok¹⁰², A. Augustinus³⁴, R. Averbach¹⁰⁴, M.D. Azmi¹⁷, A. Badalà⁵⁵, Y.W. Baek^{60,40}, S. Bagnasco⁵⁸, R. Bailhache⁶⁹, R. Bala⁹⁹, A. Baldisseri¹³⁶, M. Ball⁴², R.C. Baral⁸⁵, R. Barbera²⁸, L. Barioglio²⁶, G.G. Barnaföldi¹⁴⁴, L.S. Barnby⁹², V. Barret¹³³, P. Bartalini⁶, K. Barth³⁴, E. Bartsch⁶⁹, N. Bastid¹³³, S. Basu¹⁴², G. Batigne¹¹³, B. Batyunya⁷⁵, P.C. Batzing²¹, J.L. Bazo Alba¹⁰⁹, I.G. Bearden⁸⁸, H. Beck¹⁰², C. Bedda⁶³, N.K. Behera⁶⁰, I. Belikov¹³⁵, F. Bellini³⁴, H. Bello Martinez⁴⁴, R. Bellwied¹²⁵, L.G.E. Beltran¹¹⁹, V. Belyaev⁹¹, G. Bencedi¹⁴⁴, S. Beole²⁶, A. Bercuci⁴⁷, Y. Berdnikov⁹⁶, D. Berenyi¹⁴⁴, R.A. Bertens¹²⁹, D. Berzano^{58,34}, L. Betev³⁴, A. Bhasin⁹⁹, I.R. Bhat⁹⁹, H. Bhatt⁴⁸, B. Bhattacharjee⁴¹, J. Bhom¹¹⁷, A. Bianchi²⁶, L. Bianchi^{125,26}, N. Bianchi⁵¹, J. Bielčák³⁷, J. Bielčíková⁹³, A. Bilandzic^{103,116}, G. Biro¹⁴⁴, R. Biswas³, S. Biswas³, J.T. Blair¹¹⁸, D. Blau⁸⁷, C. Blume⁶⁹, G. Boca¹³⁸, F. Bock³⁴, A. Bogdanov⁹¹, L. Boldizsár¹⁴⁴, A. Bolozdynya⁹¹, M. Bombara³⁸, G. Bonomi¹³⁹, M. Bonora³⁴, H. Borel¹³⁶, A. Borisso^{143,102}, M. Borri¹²⁷, E. Botta²⁶, C. Bourjau⁸⁸, L. Bratrud⁶⁹, P. Braun-Munzinger¹⁰⁴, M. Bregant¹²⁰, T.A. Broker⁶⁹, M. Broz³⁷, E.J. Brucken⁴³, E. Bruna⁵⁸, G.E. Bruno³³, D. Budnikov¹⁰⁶, H. Buesching⁶⁹, S. Bufalino³¹, P. Buhler¹¹², P. Buncic³⁴, O. Busch^{132, i}, Z. Buthelezi⁷³, J.B. Butt¹⁵, J.T. Buxton⁹⁵, J. Cabala¹¹⁵, D. Caffarri⁸⁹, H. Caines¹⁴⁵, A. Caliva¹⁰⁴, E. Calvo Villar¹⁰⁹, R.S. Camacho⁴⁴, P. Camerini²⁵, A.A. Capon¹¹², F. Carnesecchi^{27,10}, J. Castillo Castellanos¹³⁶, A.J. Castro¹²⁹, E.A.R. Casula⁵⁴, C. Ceballos Sanchez⁸, S. Chandra¹⁴⁰, B. Chang¹²⁶, W. Chang⁶, S. Chapeland³⁴, M. Chartier¹²⁷, S. Chattopadhyay¹⁴⁰, S. Chattopadhyay¹⁰⁷, A. Chauvin²⁴, C. Cheshkov¹³⁴, B. Cheynis¹³⁴, V. Chibante Barroso³⁴, D.D. Chinellato¹²¹, S. Cho⁶⁰, P. Chochula³⁴, T. Chowdhury¹³³, P. Christakoglou⁸⁹, C.H. Christensen⁸⁸, P. Christiansen⁸⁰, T. Chujo¹³², C. Cicalo⁵⁴, L. Cifarelli^{10,27}, F. Cindolo⁵³, J. Cleymans¹²⁴, F. Colamaria⁵², D. Colella⁵², A. Collu⁷⁹, M. Colocci²⁷, M. Concas^{58, ii}, G. Conesa Balbastre⁷⁸, Z. Conesa del Valle⁶¹, J.G. Contreras³⁷, T.M. Cormier⁹⁴, Y. Corrales Morales⁵⁸, P. Cortese³², M.R. Cosentino¹²², F. Costa³⁴, S. Costanza¹³⁸, J. Crkovská⁶¹, P. Crochet¹³³, E. Cuautle⁷⁰, L. Cunqueiro⁹⁴, D. Dabrowski¹⁴¹, T. Dahms^{116,103}, A. Dainese⁵⁶, F.P.A. Damas^{136,113}, S. Dani⁶⁶, M.C. Danisch¹⁰², A. Danu⁶⁸, D. Das¹⁰⁷, I. Das¹⁰⁷, S. Das³, A. Dash⁸⁵, S. Dash⁴⁸, S. De⁴⁹, A. De Caro³⁰, G. de Cataldo⁵², C. de Conti¹²⁰, J. de Cuveland³⁹, A. De Falco²⁴, D. De Gruttola^{10,30}, N. De Marco⁵⁸, S. De Pasquale³⁰, R.D. De Souza¹²¹, H.F. Degenhardt¹²⁰, A. Deisting^{102,104}, A. Deloff⁸⁴, S. Delsanto²⁶, P. Dhankher⁴⁸, D. Di Bari³³, A. Di Mauro³⁴, R.A. Diaz⁸, T. Dietel¹²⁴, P. Dillenseger⁶⁹, Y. Ding⁶, R. Divià³⁴, Ø. Djuvsland²², A. Dobrin³⁴, D. Domenicis Gimenez¹²⁰, B. Dönigus⁶⁹, O. Dordic²¹, A.K. Dubey¹⁴⁰, A. Dubla¹⁰⁴, S. Dudi⁹⁸, A.K. Duggal⁹⁸, M. Dukhishyam⁸⁵, P. Dupieux¹³³, R.J. Ehlers¹⁴⁵, D. Elia⁵², H. Engel⁷⁴, E. Epple¹⁴⁵, B. Erazmus¹¹³, F. Erhardt⁹⁷, A. Erokhin¹¹¹, M.R. Ersdal²², B. Espagnon⁶¹, G. Eulisse³⁴, J. Eum¹⁸, D. Evans¹⁰⁸, S. Evdokimov⁹⁰, L. Fabbietti^{103,116}, M. Faggin²⁹, J. Faivre⁷⁸, A. Fantoni⁵¹, M. Fasel⁹⁴, L. Feldkamp¹⁴³, A. Feliciello⁵⁸, G. Feofilov¹¹¹, A. Fernández Téllez⁴⁴, A. Ferretti²⁶, A. Festanti³⁴, V.J.G. Feuillard¹⁰², J. Figiel¹¹⁷, S. Filchagin¹⁰⁶, D. Finogeev⁶², F.M. Fionda²², G. Fiorenza⁵², F. Flor¹²⁵, M. Floris³⁴, S. Foertsch⁷³, P. Foka¹⁰⁴, S. Fokin⁸⁷, E. Fragiaco⁵⁹, A. Francisco¹¹³,

U. Frankenfeld¹⁰⁴, G.G. Fronze²⁶, U. Fuchs³⁴, C. Furget⁷⁸, A. Furs⁶², M. Fusco Girard³⁰, J.J. Gaardhøje⁸⁸, M. Gagliardi²⁶, A.M. Gago¹⁰⁹, K. Gajdosova^{37,88}, C.D. Galvan¹¹⁹, P. Ganoti⁸³, C. Garabatos¹⁰⁴, E. Garcia-Solis¹¹, K. Garg²⁸, C. Gargiulo³⁴, P. Gasik^{116,103}, E.F. Gauger¹¹⁸, M.B. Gay Ducati⁷¹, M. Germain¹¹³, J. Ghosh¹⁰⁷, P. Ghosh¹⁴⁰, S.K. Ghosh³, P. Gianotti⁵¹, P. Giubellino^{104,58}, P. Giubilato²⁹, P. Glässel¹⁰², D.M. Gómez Coral⁷², A. Gomez Ramirez⁷⁴, V. Gonzalez¹⁰⁴, P. González-Zamora⁴⁴, S. Gorbunov³⁹, L. Görlich¹¹⁷, S. Gotovac³⁵, V. Grabski⁷², L.K. Graczykowski¹⁴¹, K.L. Graham¹⁰⁸, L. Greiner⁷⁹, A. Grelli⁶³, C. Grigoras³⁴, V. Grigoriev⁹¹, A. Grigoryan¹, S. Grigoryan⁷⁵, J.M. Gronefeld¹⁰⁴, F. Grosa³¹, J.F. Grosse-Oetringhaus³⁴, R. Grosso¹⁰⁴, R. Guernane⁷⁸, B. Guerzoni²⁷, M. Guittiere¹¹³, K. Gulbrandsen⁸⁸, T. Gunji¹³¹, A. Gupta⁹⁹, R. Gupta⁹⁹, I.B. Guzman⁴⁴, R. Haake^{145,34}, M.K. Habib¹⁰⁴, C. Hadjidakis⁶¹, H. Hamagaki⁸¹, G. Hamar¹⁴⁴, M. Hamid⁶, J.C. Hamon¹³⁵, R. Hannigan¹¹⁸, M.R. Haque⁶³, A. Harlenderova¹⁰⁴, J.W. Harris¹⁴⁵, A. Harton¹¹, H. Hassan⁷⁸, D. Hatzifotiadiou^{10,53}, P. Hauer⁴², S. Hayashi¹³¹, S.T. Heckel⁶⁹, E. Hellbär⁶⁹, H. Helstrup³⁶, A. Hergelegiu⁴⁷, E.G. Hernandez⁴⁴, G. Herrera Corral⁹, F. Herrmann¹⁴³, K.F. Hetland³⁶, T.E. Hilden⁴³, H. Hillemanns³⁴, C. Hills¹²⁷, B. Hippolyte¹³⁵, B. Hohlweger¹⁰³, D. Horak³⁷, S. Hornung¹⁰⁴, R. Hosokawa^{132,78}, J. Hota⁶⁶, P. Hristov³⁴, C. Huang⁶¹, C. Hughes¹²⁹, P. Huhn⁶⁹, T.J. Humanic⁹⁵, H. Hushnud¹⁰⁷, N. Hussain⁴¹, T. Hussain¹⁷, D. Hutter³⁹, D.S. Hwang¹⁹, J.P. Iddon¹²⁷, R. Ilkaev¹⁰⁶, M. Inaba¹³², M. Ippolitov⁸⁷, M.S. Islam¹⁰⁷, M. Ivanov¹⁰⁴, V. Ivanov⁹⁶, V. Izucheev⁹⁰, B. Jacak⁷⁹, N. Jacazio²⁷, P.M. Jacobs⁷⁹, M.B. Jadhav⁴⁸, S. Jadlovská¹¹⁵, J. Jadlovsky¹¹⁵, S. Jaelani⁶³, C. Jahnke^{120,116}, M.J. Jakubowska¹⁴¹, M.A. Janik¹⁴¹, M. Jercic⁹⁷, O. Jevons¹⁰⁸, R.T. Jimenez Bustamante¹⁰⁴, M. Jin¹²⁵, P.G. Jones¹⁰⁸, A. Jusko¹⁰⁸, P. Kalinak⁶⁵, A. Kalweit³⁴, J.H. Kang¹⁴⁶, V. Kaplin⁹¹, S. Kar⁶, A. Karasu Uysal⁷⁷, O. Karavichev⁶², T. Karavicheva⁶², P. Karczmarczyk³⁴, E. Karpechev⁶², U. Keschull⁷⁴, R. Keidel⁴⁶, D.L.D. Keijdener⁶³, M. Keil³⁴, B. Ketzer⁴², Z. Khabanova⁸⁹, A.M. Khan⁶, S. Khan¹⁷, S.A. Khan¹⁴⁰, A. Khanzadeev⁹⁶, Y. Kharlov⁹⁰, A. Khatun¹⁷, A. Khuntia⁴⁹, M.M. Kielbowicz¹¹⁷, B. Kileng³⁶, B. Kim⁶⁰, B. Kim¹³², D. Kim¹⁴⁶, D.J. Kim¹²⁶, E.J. Kim¹³, H. Kim¹⁴⁶, J.S. Kim⁴⁰, J. Kim¹⁰², J. Kim¹³, M. Kim^{60,102}, S. Kim¹⁹, T. Kim¹⁴⁶, T. Kim¹⁴⁶, K. Kindra⁹⁸, S. Kirsch³⁹, I. Kisel³⁹, S. Kiselev⁶⁴, A. Kisiel¹⁴¹, J.L. Klay⁵, C. Klein⁶⁹, J. Klein⁵⁸, C. Klein-Bösing¹⁴³, S. Klewin¹⁰², A. Kluge³⁴, M.L. Knichel³⁴, A.G. Knospe¹²⁵, C. Kobdaj¹¹⁴, M. Kofarago¹⁴⁴, M.K. Köhler¹⁰², T. Kollegger¹⁰⁴, N. Kondratyeva⁹¹, E. Kondratyuk⁹⁰, A. Konevskikh⁶², P.J. Konopka³⁴, M. Konyushikhin¹⁴², L. Koska¹¹⁵, O. Kovalenko⁸⁴, V. Kovalenko¹¹¹, M. Kowalski¹¹⁷, I. Králik⁶⁵, A. Kravčáková³⁸, L. Kreis¹⁰⁴, M. Krivda^{108,65}, F. Krizek⁹³, M. Krüger⁶⁹, E. Kryshen⁹⁶, M. Krzewicki³⁹, A.M. Kubera⁹⁵, V. Kučera^{93,60}, C. Kuhn¹³⁵, P.G. Kuijer⁸⁹, J. Kumar⁴⁸, L. Kumar⁹⁸, S. Kumar⁴⁸, S. Kundu⁸⁵, P. Kurashvili⁸⁴, A. Kurepin⁶², A.B. Kurepin⁶², S. Kushpil⁹³, J. Kvapil¹⁰⁸, M.J. Kweon⁶⁰, Y. Kwon¹⁴⁶, S.L. La Pointe³⁹, P. La Rocca²⁸, Y.S. Lai⁷⁹, I. Lakomov³⁴, R. Langoy¹²³, K. Lapidus^{145,34}, A. Lardeux²¹, P. Larionov⁵¹, E. Laudi³⁴, R. Lavicka³⁷, T. Lazareva¹¹¹, R. Lea²⁵, L. Leardini¹⁰², S. Lee¹⁴⁶, F. Lehas⁸⁹, S. Lehner¹¹², J. Lehrbach³⁹, R.C. Lemmon⁹², I. León Monzón¹¹⁹, P. Lévai¹⁴⁴, X. Li¹², X.L. Li⁶, J. Lien¹²³, R. Lietava¹⁰⁸, B. Lim¹⁸, S. Lindal²¹, V. Lindenstruth³⁹, S.W. Lindsay¹²⁷, C. Lippmann¹⁰⁴, M.A. Lisa⁹⁵, V. Litichevskiy⁴³, A. Liu⁷⁹, H.M. Ljunggren⁸⁰, W.J. Llope¹⁴², D.F. Lodato⁶³, V. Loginov⁹¹, C. Loizides⁹⁴, P. Loncar³⁵, X. Lopez¹³³, E. López Torres⁸, P. Luettig⁶⁹, J.R. Luhder¹⁴³, M. Lunardon²⁹, G. Luparello⁵⁹, M. Lupi³⁴, A. Maevskaya⁶², M. Mager³⁴, S.M. Mahmood²¹, A. Maire¹³⁵, R.D. Majka¹⁴⁵, M. Malaev⁹⁶, Q.W. Malik²¹, L. Malinina^{75,iii}, D. Mal'Kevich⁶⁴, P. Malzacher¹⁰⁴, A. Mamonov¹⁰⁶, V. Manko⁸⁷, F. Manso¹³³, V. Manzari⁵², Y. Mao⁶, M. Marchisone¹³⁴, J. Mareš⁶⁷, G.V. Margagliotti²⁵, A. Margotti⁵³, J. Margutti⁶³, A. Marín¹⁰⁴, C. Markert¹¹⁸, M. Marquard⁶⁹, N.A. Martin^{102,104}, P. Martinengo³⁴, J.L. Martinez¹²⁵, M.I. Martínez⁴⁴, G. Martínez García¹¹³, M. Martinez Pedreira³⁴, S. Masciocchi¹⁰⁴, M. Maserà²⁶, A. Masoni⁵⁴, L. Massacrier⁶¹, E. Masson¹¹³, A. Mastroserio^{137,52}, A.M. Mathis^{116,103},

P.F.T. Matuoka¹²⁰, A. Matyja^{117,129}, C. Mayer¹¹⁷, M. Mazzilli³³, M.A. Mazzoni⁵⁷, F. Meddi²³, Y. Melikyan⁹¹, A. Menchaca-Rocha⁷², E. Meninno³⁰, M. Meres¹⁴, S. Mhlanga¹²⁴, Y. Miake¹³², L. Micheletti²⁶, M.M. Mieskolainen⁴³, D.L. Mihaylov¹⁰³, K. Mikhaylov^{75,64}, A. Mischke⁶³, A.N. Mishra⁷⁰, D. Miśkowiec¹⁰⁴, J. Mitra¹⁴⁰, C.M. Mitu⁶⁸, N. Mohammadi³⁴, A.P. Mohanty⁶³, B. Mohanty⁸⁵, M. Mohisin Khan^{17, iv}, M.M. Mondal⁶⁶, D.A. Moreira De Godoy¹⁴³, L.A.P. Moreno⁴⁴, S. Moretto²⁹, A. Morreale¹¹³, A. Morsch³⁴, T. Mrnjavac³⁴, V. Muccifora⁵¹, E. Mudnic³⁵, D. Mühlheim¹⁴³, S. Muhuri¹⁴⁰, J.D. Mulligan¹⁴⁵, M.G. Munhoz¹²⁰, K. Mürning⁴², M.I.A. Muñoz⁷⁹, R.H. Munzer⁶⁹, H. Murakami¹³¹, S. Murray⁷³, L. Musa³⁴, J. Musinsky⁶⁵, C.J. Myers¹²⁵, J.W. Myrcha¹⁴¹, B. Naik⁴⁸, R. Nair⁸⁴, B.K. Nandi⁴⁸, R. Nania^{53,10}, E. Nappi⁵², M.U. Naru¹⁵, A.F. Nassirpour⁸⁰, H. Natal da Luz¹²⁰, C. Natrass¹²⁹, S.R. Navarro⁴⁴, K. Nayak⁸⁵, R. Nayak⁴⁸, T.K. Nayak^{140,85}, S. Nazarenko¹⁰⁶, R.A. Negrao De Oliveira⁶⁹, L. Nellen⁷⁰, S.V. Nesbo³⁶, G. Neskovic³⁹, F. Ng¹²⁵, J. Niedziela^{141,34}, B.S. Nielsen⁸⁸, S. Nikolaev⁸⁷, S. Nikulin⁸⁷, V. Nikulin⁹⁶, F. Noferini^{10,53}, P. Nomokonov⁷⁵, G. Nooren⁶³, J.C.C. Noris⁴⁴, J. Norman⁷⁸, A. Nyanin⁸⁷, J. Nystrand²², M. Ogino⁸¹, A. Ohlson¹⁰², J. Oleniacz¹⁴¹, A.C. Oliveira Da Silva¹²⁰, M.H. Oliver¹⁴⁵, J. Onderwaater¹⁰⁴, C. Oppedisano⁵⁸, R. Orava⁴³, M. Oravec¹¹⁵, A. Ortiz Velasquez⁷⁰, A. Oskarsson⁸⁰, J. Otwinowski¹¹⁷, K. Oyama⁸¹, Y. Pachmayer¹⁰², V. Pacik⁸⁸, D. Pagano¹³⁹, G. Paic⁷⁰, P. Palmi⁶, J. Pan¹⁴², A.K. Pandey⁴⁸, S. Panebianco¹³⁶, V. Papikyan¹, P. Pareek⁴⁹, J. Park⁶⁰, J.E. Parkkila¹²⁶, S. Parmar⁹⁸, A. Passfeld¹⁴³, S.P. Pathak¹²⁵, R.N. Patra¹⁴⁰, B. Paul⁵⁸, H. Pei⁶, T. Peitzmann⁶³, X. Peng⁶, L.G. Pereira⁷¹, H. Pereira Da Costa¹³⁶, D. Peresunko⁸⁷, E. Perez Lezama⁶⁹, V. Peskov⁶⁹, Y. Pestov⁴, V. Petráček³⁷, M. Petrovici⁴⁷, R.P. Pezzi⁷¹, S. Piano⁵⁹, M. Pikna¹⁴, P. Pillot¹¹³, L.O.D.L. Pimentel⁸⁸, O. Pinazza^{53,34}, L. Pinsky¹²⁵, S. Pisano⁵¹, D.B. Piyarathna¹²⁵, M. Płoskoń⁷⁹, M. Planinic⁹⁷, F. Pliquett⁶⁹, J. Pluta¹⁴¹, S. Pochybova¹⁴⁴, P.L.M. Podesta-Lerma¹¹⁹, M.G. Poghosyan⁹⁴, B. Polichtchouk⁹⁰, N. Poljak⁹⁷, W. Poonsawat¹¹⁴, A. Pop⁴⁷, H. Poppenborg¹⁴³, S. Porteboeuf-Houssais¹³³, V. Pozdniakov⁷⁵, S.K. Prasad³, R. Preghenella⁵³, F. Prino⁵⁸, C.A. Pruneau¹⁴², I. Pshenichnov⁶², M. Puccio²⁶, V. Punin¹⁰⁶, K. Puranapanda¹⁴⁰, J. Putschke¹⁴², R.E. Quishpe¹²⁵, S. Raha³, S. Rajput⁹⁹, J. Rak¹²⁶, A. Rakotozafindrabe¹³⁶, L. Ramello³², F. Rami¹³⁵, R. Raniwala¹⁰⁰, S. Raniwala¹⁰⁰, S.S. Räsänen⁴³, B.T. Rascanu⁶⁹, R. Rath⁴⁹, V. Ratzka⁴², I. Ravasenga³¹, K.F. Read^{94,129}, K. Redlich^{84, v}, A. Rehman²², P. Reichelt⁶⁹, F. Reidt³⁴, X. Ren⁶, R. Renfordt⁶⁹, A. Reshetin⁶², J.-P. Revol¹⁰, K. Reygers¹⁰², V. Riabov⁹⁶, T. Richert^{88,80}, M. Richter²¹, P. Riedler³⁴, W. Riegler³⁴, F. Riggi²⁸, C. Ristea⁶⁸, S.P. Rode⁴⁹, M. Rodríguez Cahuantzi⁴⁴, K. Røed²¹, R. Rogalev⁹⁰, E. Rogochaya⁷⁵, D. Rohr³⁴, D. Röhrich²², P.S. Rokita¹⁴¹, F. Ronchetti⁵¹, E.D. Rosas⁷⁰, K. Roslon¹⁴¹, P. Rosnet¹³³, A. Rossi^{56,29}, A. Rotondi¹³⁸, F. Roukoutakis⁸³, A. Roy⁴⁹, P. Roy¹⁰⁷, O.V. Rueda⁷⁰, R. Rui²⁵, B. Rumyantsev⁷⁵, A. Rustamov⁸⁶, E. Ryabinkin⁸⁷, Y. Ryabov⁹⁶, A. Rybicki¹¹⁷, S. Saarinen⁴³, S. Sadhu¹⁴⁰, S. Sadovsky⁹⁰, K. Šafařík³⁴, S.K. Saha¹⁴⁰, B. Sahoo⁴⁸, P. Sahoo⁴⁹, R. Sahoo⁴⁹, S. Sahoo⁶⁶, P.K. Sahu⁶⁶, J. Saini¹⁴⁰, S. Sakai¹³², M.A. Saleh¹⁴², S. Sambyal⁹⁹, V. Samsonov^{91,96}, A. Sandoval⁷², A. Sarkar⁷³, D. Sarkar¹⁴⁰, N. Sarkar¹⁴⁰, P. Sarma⁴¹, M.H.P. Sas⁶³, E. Scapparone⁵³, B. Schaefer⁹⁴, J. Schambach¹¹⁸, H.S. Scheid⁶⁹, C. Schiaua⁴⁷, R. Schicker¹⁰², C. Schmidt¹⁰⁴, H.R. Schmidt¹⁰¹, M.O. Schmidt¹⁰², M. Schmidt¹⁰¹, N.V. Schmidt^{94,69}, J. Schukraft^{34,88}, Y. Schutz^{34,135}, K. Schwarz¹⁰⁴, K. Schweda¹⁰⁴, G. Scioli²⁷, E. Scomparin⁵⁸, M. Šefčík³⁸, J.E. Seger¹⁶, Y. Sekiguchi¹³¹, D. Sekihata⁴⁵, I. Selyuzhenkov^{91,104}, S. Senyukov¹³⁵, E. Serradilla⁷², P. Sett⁴⁸, A. Sevcenco⁶⁸, A. Shabanov⁶², A. Shabetai¹¹³, R. Shahoyan³⁴, W. Shaikh¹⁰⁷, A. Shangaraev⁹⁰, A. Sharma⁹⁸, A. Sharma⁹⁹, M. Sharma⁹⁹, N. Sharma⁹⁸, A.I. Sheikh¹⁴⁰, K. Shigaki⁴⁵, M. Shimomura⁸², S. Shirinkin⁶⁴, Q. Shou^{6,110}, Y. Sibiriak⁸⁷, S. Siddhanta⁵⁴, T. Siemiarczuk⁸⁴, D. Silvermyr⁸⁰, G. Simatovic⁸⁹, G. Simonetti^{103,34}, R. Singh⁸⁵, R. Singh⁹⁹, V. Singhal¹⁴⁰, T. Sinha¹⁰⁷, B. Sitar¹⁴, M. Sitta³², T.B. Skaali²¹, M. Slupecki¹²⁶, N. Smirnov¹⁴⁵,

R.J.M. Snellings⁶³, T.W. Snellman¹²⁶, J. Sochan¹¹⁵, C. Soncco¹⁰⁹, J. Song⁶⁰, A. Songmoolnak¹¹⁴, F. Soramel²⁹, S. Sorensen¹²⁹, F. Sozzi¹⁰⁴, I. Sputowska¹¹⁷, J. Stachel¹⁰², I. Stan⁶⁸, P. Stankus⁹⁴, E. Stenlund⁸⁰, D. Stocco¹¹³, M.M. Storetvedt³⁶, P. Strmen¹⁴, A.A.P. Suaide¹²⁰, T. Sugitate⁴⁵, C. Suire⁶¹, M. Suleymanov¹⁵, M. Suljic³⁴, R. Sultanov⁶⁴, M. Šumbera⁹³, S. Sumowidagdo⁵⁰, K. Suzuki¹¹², S. Swain⁶⁶, A. Szabo¹⁴, I. Szarka¹⁴, U. Tabassam¹⁵, J. Takahashi¹²¹, G.J. Tambave²², N. Tanaka¹³², M. Tarhini¹¹³, M.G. Tarzila⁴⁷, A. Tauro³⁴, G. Tejada Muñoz⁴⁴, A. Telesca³⁴, C. Terrevoli^{125,29}, D. Thakur⁴⁹, S. Thakur¹⁴⁰, D. Thomas¹¹⁸, F. Thoresen⁸⁸, R. Tieulent¹³⁴, A. Tikhonov⁶², A.R. Timmins¹²⁵, A. Toia⁶⁹, N. Topilskaya⁶², M. Toppi⁵¹, F. Torales-Acosta²⁰, S.R. Torres¹¹⁹, S. Tripathy⁴⁹, S. Trogolo²⁶, G. Trombetta³³, L. Tropp³⁸, V. Trubnikov², W.H. Trzaska¹²⁶, T.P. Trzcinski¹⁴¹, B.A. Trzeciak⁶³, T. Tsuji¹³¹, A. Tumkin¹⁰⁶, R. Turrisi⁵⁶, T.S. Tveter²¹, K. Ullaland²², E.N. Umaka¹²⁵, A. Uras¹³⁴, G.L. Usai²⁴, A. Utrobicic⁹⁷, M. Vala^{38,115}, L. Valencia Palomo⁴⁴, N. Valle¹³⁸, N. van der Kolk⁶³, L.V.R. van Doremalen⁶³, J.W. Van Hoorne³⁴, M. van Leeuwen⁶³, P. Vande Vyvre³⁴, D. Varga¹⁴⁴, A. Vargas⁴⁴, M. Vargyas¹²⁶, R. Varma⁴⁸, M. Vasileiou⁸³, A. Vasiliev⁸⁷, O. Vázquez Doce^{103,116}, V. Vechernin¹¹¹, A.M. Veen⁶³, E. Vercellin²⁶, S. Vergara Limón⁴⁴, L. Vermunt⁶³, R. Vernet⁷, R. Vértesi¹⁴⁴, L. Vickovic³⁵, J. Viinikainen¹²⁶, Z. Vilakazi¹³⁰, O. Villalobos Baillie¹⁰⁸, A. Villatoro Tello⁴⁴, G. Vino⁵², A. Vinogradov⁸⁷, T. Virgili³⁰, V. Vislavicius^{80,88}, A. Vodopyanov⁷⁵, B. Volkel³⁴, M.A. Völkl¹⁰¹, K. Voloshin⁶⁴, S.A. Voloshin¹⁴², G. Volpe³³, B. von Haller³⁴, I. Vorobyev^{116,103}, D. Voscek¹¹⁵, J. Vrláková³⁸, B. Wagner²², M. Wang⁶, Y. Watanabe¹³², M. Weber¹¹², S.G. Weber¹⁰⁴, A. Wegrzynek³⁴, D.F. Weiser¹⁰², S.C. Wenzel³⁴, J.P. Wessels¹⁴³, U. Westerhoff¹⁴³, A.M. Whitehead¹²⁴, E. Widmann¹¹², J. Wiechula⁶⁹, J. Wikne²¹, G. Wilk⁸⁴, J. Wilkinson⁵³, G.A. Willems^{143,34}, E. Willsher¹⁰⁸, B. Windelband¹⁰², W.E. Witt¹²⁹, Y. Wu¹²⁸, R. Xu⁶, S. Yalcin⁷⁷, K. Yamakawa⁴⁵, S. Yano^{136,45}, Z. Yin⁶, H. Yokoyama^{63,132,78}, I.-K. Yoo¹⁸, J.H. Yoon⁶⁰, S. Yuan²², V. Yurchenko², V. Zaccolo⁵⁸, A. Zaman¹⁵, C. Zampolli³⁴, H.J.C. Zanoli¹²⁰, N. Zardoshti¹⁰⁸, A. Zarochentsev¹¹¹, P. Závada⁶⁷, N. Zaviyalov¹⁰⁶, H. Zbroszczyk¹⁴¹, M. Zhalov⁹⁶, X. Zhang⁶, Y. Zhang⁶, Z. Zhang^{133,6}, C. Zhao²¹, V. Zherebchevskii¹¹¹, N. Zhigareva⁶⁴, D. Zhou⁶, Y. Zhou⁸⁸, Z. Zhou²², H. Zhu⁶, J. Zhu⁶, Y. Zhu⁶, A. Zichichi^{10,27}, M.B. Zimmermann³⁴, G. Zinovjev²

ⁱ Deceased

ⁱⁱ Dipartimento DET del Politecnico di Torino, Turin, Italy

ⁱⁱⁱ M.V. Lomonosov Moscow State University, D.V. Skobeltsyn Institute of Nuclear, Physics, Moscow, Russia

^{iv} Department of Applied Physics, Aligarh Muslim University, Aligarh, India

^v Institute of Theoretical Physics, University of Wrocław, Poland

¹ A.I. Alikhanyan National Science Laboratory (Yerevan Physics Institute) Foundation, Yerevan, Armenia

² Bogolyubov Institute for Theoretical Physics, National Academy of Sciences of Ukraine, Kiev, Ukraine

³ Bose Institute, Department of Physics and Centre for Astroparticle Physics and Space Science (CAPSS), Kolkata, India

⁴ Budker Institute for Nuclear Physics, Novosibirsk, Russia

⁵ California Polytechnic State University, San Luis Obispo, California, United States

⁶ Central China Normal University, Wuhan, China

⁷ Centre de Calcul de l'IN2P3, Villeurbanne, Lyon, France

⁸ Centro de Aplicaciones Tecnológicas y Desarrollo Nuclear (CEADEN), Havana, Cuba

⁹ Centro de Investigación y de Estudios Avanzados (CINVESTAV), Mexico City and Mérida, Mexico

¹⁰ Centro Fermi - Museo Storico della Fisica e Centro Studi e Ricerche "Enrico Fermi", Rome, Italy

- 11 *Chicago State University, Chicago, Illinois, United States*
- 12 *China Institute of Atomic Energy, Beijing, China*
- 13 *Chonbuk National University, Jeonju, Republic of Korea*
- 14 *Comenius University Bratislava, Faculty of Mathematics, Physics and Informatics, Bratislava, Slovakia*
- 15 *COMSATS Institute of Information Technology (CIIT), Islamabad, Pakistan*
- 16 *Creighton University, Omaha, Nebraska, United States*
- 17 *Department of Physics, Aligarh Muslim University, Aligarh, India*
- 18 *Department of Physics, Pusan National University, Pusan, Republic of Korea*
- 19 *Department of Physics, Sejong University, Seoul, Republic of Korea*
- 20 *Department of Physics, University of California, Berkeley, California, United States*
- 21 *Department of Physics, University of Oslo, Oslo, Norway*
- 22 *Department of Physics and Technology, University of Bergen, Bergen, Norway*
- 23 *Dipartimento di Fisica dell'Università 'La Sapienza' and Sezione INFN, Rome, Italy*
- 24 *Dipartimento di Fisica dell'Università and Sezione INFN, Cagliari, Italy*
- 25 *Dipartimento di Fisica dell'Università and Sezione INFN, Trieste, Italy*
- 26 *Dipartimento di Fisica dell'Università and Sezione INFN, Turin, Italy*
- 27 *Dipartimento di Fisica e Astronomia dell'Università and Sezione INFN, Bologna, Italy*
- 28 *Dipartimento di Fisica e Astronomia dell'Università and Sezione INFN, Catania, Italy*
- 29 *Dipartimento di Fisica e Astronomia dell'Università and Sezione INFN, Padova, Italy*
- 30 *Dipartimento di Fisica 'E.R. Caianiello' dell'Università and Gruppo Collegato INFN, Salerno, Italy*
- 31 *Dipartimento DISAT del Politecnico and Sezione INFN, Turin, Italy*
- 32 *Dipartimento di Scienze e Innovazione Tecnologica dell'Università del Piemonte Orientale and INFN Sezione di Torino, Alessandria, Italy*
- 33 *Dipartimento Interateneo di Fisica 'M. Merlin' and Sezione INFN, Bari, Italy*
- 34 *European Organization for Nuclear Research (CERN), Geneva, Switzerland*
- 35 *Faculty of Electrical Engineering, Mechanical Engineering and Naval Architecture, University of Split, Split, Croatia*
- 36 *Faculty of Engineering and Science, Western Norway University of Applied Sciences, Bergen, Norway*
- 37 *Faculty of Nuclear Sciences and Physical Engineering, Czech Technical University in Prague, Prague, Czech Republic*
- 38 *Faculty of Science, P.J. Šafárik University, Košice, Slovakia*
- 39 *Frankfurt Institute for Advanced Studies, Johann Wolfgang Goethe-Universität Frankfurt, Frankfurt, Germany*
- 40 *Gangneung-Wonju National University, Gangneung, Republic of Korea*
- 41 *Gauhati University, Department of Physics, Guwahati, India*
- 42 *Helmholtz-Institut für Strahlen- und Kernphysik, Rheinische Friedrich-Wilhelms-Universität Bonn, Bonn, Germany*
- 43 *Helsinki Institute of Physics (HIP), Helsinki, Finland*
- 44 *High Energy Physics Group, Universidad Autónoma de Puebla, Puebla, Mexico*
- 45 *Hiroshima University, Hiroshima, Japan*
- 46 *Hochschule Worms, Zentrum für Technologietransfer und Telekommunikation (ZTT), Worms, Germany*
- 47 *Horia Hulubei National Institute of Physics and Nuclear Engineering, Bucharest, Romania*
- 48 *Indian Institute of Technology Bombay (IIT), Mumbai, India*
- 49 *Indian Institute of Technology Indore, Indore, India*
- 50 *Indonesian Institute of Sciences, Jakarta, Indonesia*
- 51 *INFN, Laboratori Nazionali di Frascati, Frascati, Italy*
- 52 *INFN, Sezione di Bari, Bari, Italy*
- 53 *INFN, Sezione di Bologna, Bologna, Italy*
- 54 *INFN, Sezione di Cagliari, Cagliari, Italy*

- 55 INFN, Sezione di Catania, Catania, Italy
- 56 INFN, Sezione di Padova, Padova, Italy
- 57 INFN, Sezione di Roma, Rome, Italy
- 58 INFN, Sezione di Torino, Turin, Italy
- 59 INFN, Sezione di Trieste, Trieste, Italy
- 60 Inha University, Incheon, Republic of Korea
- 61 Institut de Physique Nucléaire d'Orsay (IPNO), Institut National de Physique Nucléaire et de Physique des Particules (IN2P3/CNRS), Université de Paris-Sud, Université Paris-Saclay, Orsay, France
- 62 Institute for Nuclear Research, Academy of Sciences, Moscow, Russia
- 63 Institute for Subatomic Physics, Utrecht University/Nikhef, Utrecht, Netherlands
- 64 Institute for Theoretical and Experimental Physics, Moscow, Russia
- 65 Institute of Experimental Physics, Slovak Academy of Sciences, Košice, Slovakia
- 66 Institute of Physics, Homi Bhabha National Institute, Bhubaneswar, India
- 67 Institute of Physics of the Czech Academy of Sciences, Prague, Czech Republic
- 68 Institute of Space Science (ISS), Bucharest, Romania
- 69 Institut für Kernphysik, Johann Wolfgang Goethe-Universität Frankfurt, Frankfurt, Germany
- 70 Instituto de Ciencias Nucleares, Universidad Nacional Autónoma de México, Mexico City, Mexico
- 71 Instituto de Física, Universidade Federal do Rio Grande do Sul (UFRGS), Porto Alegre, Brazil
- 72 Instituto de Física, Universidad Nacional Autónoma de México, Mexico City, Mexico
- 73 iThemba LABS, National Research Foundation, Somerset West, South Africa
- 74 Johann-Wolfgang-Goethe Universität Frankfurt Institut für Informatik, Fachbereich Informatik und Mathematik, Frankfurt, Germany
- 75 Joint Institute for Nuclear Research (JINR), Dubna, Russia
- 76 Korea Institute of Science and Technology Information, Daejeon, Republic of Korea
- 77 KTO Karatay University, Konya, Turkey
- 78 Laboratoire de Physique Subatomique et de Cosmologie, Université Grenoble-Alpes, CNRS-IN2P3, Grenoble, France
- 79 Lawrence Berkeley National Laboratory, Berkeley, California, United States
- 80 Lund University Department of Physics, Division of Particle Physics, Lund, Sweden
- 81 Nagasaki Institute of Applied Science, Nagasaki, Japan
- 82 Nara Women's University (NWU), Nara, Japan
- 83 National and Kapodistrian University of Athens, School of Science, Department of Physics , Athens, Greece
- 84 National Centre for Nuclear Research, Warsaw, Poland
- 85 National Institute of Science Education and Research, Homi Bhabha National Institute, Jatni, India
- 86 National Nuclear Research Center, Baku, Azerbaijan
- 87 National Research Centre Kurchatov Institute, Moscow, Russia
- 88 Niels Bohr Institute, University of Copenhagen, Copenhagen, Denmark
- 89 Nikhef, National institute for subatomic physics, Amsterdam, Netherlands
- 90 NRC Kurchatov Institute IHEP, Protvino, Russia
- 91 NRNU Moscow Engineering Physics Institute, Moscow, Russia
- 92 Nuclear Physics Group, STFC Daresbury Laboratory, Daresbury, United Kingdom
- 93 Nuclear Physics Institute of the Czech Academy of Sciences, Řež u Prahy, Czech Republic
- 94 Oak Ridge National Laboratory, Oak Ridge, Tennessee, United States
- 95 Ohio State University, Columbus, Ohio, United States
- 96 Petersburg Nuclear Physics Institute, Gatchina, Russia
- 97 Physics department, Faculty of science, University of Zagreb, Zagreb, Croatia
- 98 Physics Department, Panjab University, Chandigarh, India
- 99 Physics Department, University of Jammu, Jammu, India
- 100 Physics Department, University of Rajasthan, Jaipur, India
- 101 Physikalisches Institut, Eberhard-Karls-Universität Tübingen, Tübingen, Germany

- 102 *Physikalisches Institut, Ruprecht-Karls-Universität Heidelberg, Heidelberg, Germany*
 103 *Physik Department, Technische Universität München, Munich, Germany*
 104 *Research Division and ExtreMe Matter Institute EMMI, GSI Helmholtzzentrum für
Schwerionenforschung GmbH, Darmstadt, Germany*
 105 *Rudjer Bošković Institute, Zagreb, Croatia*
 106 *Russian Federal Nuclear Center (VNIIEF), Sarov, Russia*
 107 *Saha Institute of Nuclear Physics, Homi Bhabha National Institute, Kolkata, India*
 108 *School of Physics and Astronomy, University of Birmingham, Birmingham, United Kingdom*
 109 *Sección Física, Departamento de Ciencias, Pontificia Universidad Católica del Perú, Lima, Peru*
 110 *Shanghai Institute of Applied Physics, Shanghai, China*
 111 *St. Petersburg State University, St. Petersburg, Russia*
 112 *Stefan Meyer Institut für Subatomare Physik (SMI), Vienna, Austria*
 113 *SUBATECH, IMT Atlantique, Université de Nantes, CNRS-IN2P3, Nantes, France*
 114 *Suranaree University of Technology, Nakhon Ratchasima, Thailand*
 115 *Technical University of Košice, Košice, Slovakia*
 116 *Technische Universität München, Excellence Cluster ‘Universe’, Munich, Germany*
 117 *The Henryk Niewodniczanski Institute of Nuclear Physics, Polish Academy of Sciences, Cracow,
Poland*
 118 *The University of Texas at Austin, Austin, Texas, United States*
 119 *Universidad Autónoma de Sinaloa, Culiacán, Mexico*
 120 *Universidade de São Paulo (USP), São Paulo, Brazil*
 121 *Universidade Estadual de Campinas (UNICAMP), Campinas, Brazil*
 122 *Universidade Federal do ABC, Santo Andre, Brazil*
 123 *University College of Southeast Norway, Tonsberg, Norway*
 124 *University of Cape Town, Cape Town, South Africa*
 125 *University of Houston, Houston, Texas, United States*
 126 *University of Jyväskylä, Jyväskylä, Finland*
 127 *University of Liverpool, Liverpool, United Kingdom*
 128 *University of Science and Technology of China, Hefei, China*
 129 *University of Tennessee, Knoxville, Tennessee, United States*
 130 *University of the Witwatersrand, Johannesburg, South Africa*
 131 *University of Tokyo, Tokyo, Japan*
 132 *University of Tsukuba, Tsukuba, Japan*
 133 *Université Clermont Auvergne, CNRS/IN2P3, LPC, Clermont-Ferrand, France*
 134 *Université de Lyon, Université Lyon 1, CNRS/IN2P3, IPN-Lyon, Villeurbanne, Lyon, France*
 135 *Université de Strasbourg, CNRS, IPHC UMR 7178, F-67000 Strasbourg, France, Strasbourg, France*
 136 *Université Paris-Saclay Centre d’Études de Saclay (CEA), IRFU, Department de Physique
Nucléaire (DPhN), Saclay, France*
 137 *Università degli Studi di Foggia, Foggia, Italy*
 138 *Università degli Studi di Pavia, Pavia, Italy*
 139 *Università di Brescia, Brescia, Italy*
 140 *Variable Energy Cyclotron Centre, Homi Bhabha National Institute, Kolkata, India*
 141 *Warsaw University of Technology, Warsaw, Poland*
 142 *Wayne State University, Detroit, Michigan, United States*
 143 *Westfälische Wilhelms-Universität Münster, Institut für Kernphysik, Münster, Germany*
 144 *Wigner Research Centre for Physics, Hungarian Academy of Sciences, Budapest, Hungary*
 145 *Yale University, New Haven, Connecticut, United States*
 146 *Yonsei University, Seoul, Republic of Korea*